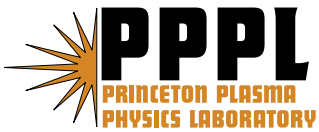

Princeton Plasma Physics Laboratory

PPPL-

PPPL-



Prepared for the U.S. Department of Energy under Contract DE-AC02-76CH03073.

Princeton Plasma Physics Laboratory

Report Disclaimers

Full Legal Disclaimer

This report was prepared as an account of work sponsored by an agency of the United States Government. Neither the United States Government nor any agency thereof, nor any of their employees, nor any of their contractors, subcontractors or their employees, makes any warranty, express or implied, or assumes any legal liability or responsibility for the accuracy, completeness, or any third party's use or the results of such use of any information, apparatus, product, or process disclosed, or represents that its use would not infringe privately owned rights. Reference herein to any specific commercial product, process, or service by trade name, trademark, manufacturer, or otherwise, does not necessarily constitute or imply its endorsement, recommendation, or favoring by the United States Government or any agency thereof or its contractors or subcontractors. The views and opinions of authors expressed herein do not necessarily state or reflect those of the United States Government or any agency thereof.

Trademark Disclaimer

Reference herein to any specific commercial product, process, or service by trade name, trademark, manufacturer, or otherwise, does not necessarily constitute or imply its endorsement, recommendation, or favoring by the United States Government or any agency thereof or its contractors or subcontractors.

PPPL Report Availability

Princeton Plasma Physics Laboratory:

<http://www.pppl.gov/techreports.cfm>

Office of Scientific and Technical Information (OSTI):

<http://www.osti.gov/bridge>

Related Links:

[U.S. Department of Energy](#)

[Office of Scientific and Technical Information](#)

[Fusion Links](#)

The remarkable similarity between the scaling of kurtosis with squared skewness for TORPEX density fluctuations and sea-surface temperature fluctuations

John A. Krommes*

Plasma Physics Laboratory, Princeton University,
P.O. Box 451, MS 28, Princeton, NJ 08543-0451

(Dated: February 15, 2008)

The striking similarity between the statistics of plasma density fluctuations in the TORPEX device [B. Labit *et al.*, Phys. Rev. Lett. **98**, 255002 (2007)] and sea-surface temperature fluctuations [P. Sura and P. D. Sardeshmukh, J. Phys. Oceanogr. **38**, 638 (2007)] (SS) is discussed. A nonlinear Langevin theory due to SS is generalized to include linear wave propagation. An interpretation of the nonlinear Langevin equation based on statistical closure theory is proposed.

Labit *et al.*^{1,2} have compiled a database of experimental shots in the TORPEX device that embraces regimes of both drift-interchange (D-I) turbulence and intermittent blobs. They found that the kurtosis K depends parabolically on the skewness S : $K = aS^2 + b$, with $a \approx 1.5$ and $b \approx -0.22$; see Fig. 1. [For a centered random variable (r.v.) \tilde{x} (tilde denotes a r.v.) with variance σ^2 , $S \doteq \langle \tilde{x}^3 \rangle / \sigma^3$ (\doteq denotes a definition) and $K \doteq F - 3$, where the flatness is $F \doteq \langle \tilde{x}^4 \rangle / \sigma^4$.] Remarkably, essentially the same relation has been shown to hold in a global database of sea-surface temperature (SST) fluctuations³; see Fig. 2. Sura and Sardeshmukh (SS) have proposed a nonlinear Langevin (L) model³ that predicts $a = \frac{3}{2}$ and $b = 0$, an obvious success. I shall discuss the possibility of generalizing the SS model to include linear waves, an essential feature of D-I turbulence, and I discuss an interpretation of the model for situations in which fluctuations are self-generated rather than forced externally.

Higher-order statistics provide a substantial challenge for conventional cumulant-based statistical closures.⁴⁻⁶ A realizability constraint is $K \geq S^2 - 2$, but detailed calculations of such statistics from, e.g., the direct-interaction approximation (DIA) are very difficult; furthermore, cer-

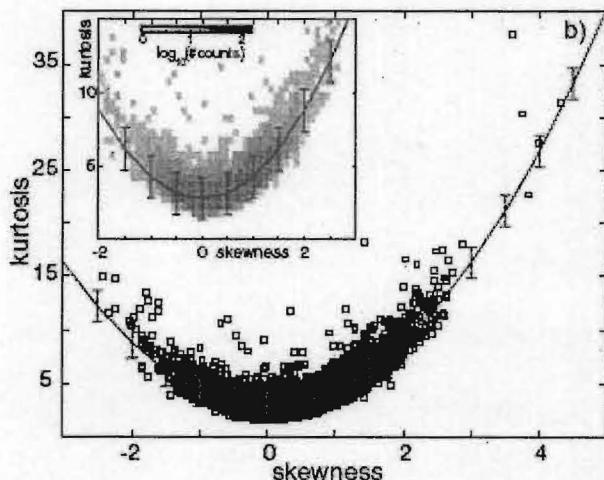


FIG. 1: Flatness $F \doteq K + 3$ (called “kurtosis” on the ordinate) versus skewness S for 8966 shots in TORPEX. Figure reprinted with permission from Ref. 1, Fig. 1, copyright 2007 by the American Physical Society.

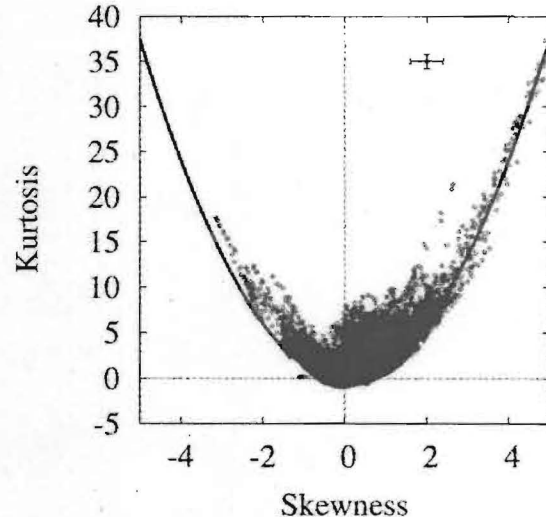


FIG. 2: Kurtosis K versus skewness S for a global database of fluctuations in sea-surface temperature. Solid line: $K = \frac{3}{2}S^2$. Figure reprinted with permission from Ref. 3, Fig. 3, copyright 2007 by the American Meteorological Society.

tain fourth-order statistics are not correctly predicted by the DIA⁵ and its Markovian relatives.⁶ Yet even very simple models can exhibit nontrivial relationships between K and S . For example, consider the r.v. $\tilde{\Gamma} \doteq \tilde{x}\tilde{y}$, where \tilde{x} and \tilde{y} are jointly Gaussian with correlation coefficient ρ . The probability density function (PDF) $P(\Gamma)$ is known⁷ (see Fig. 3) and from that $S_\Gamma(\rho)$ and $K_\Gamma(\rho)$ can be found. A parametric plot of their relation (not shown) reveals that $K_\Gamma \approx a_\Gamma S_\Gamma^2 + b_\Gamma$ with $a_\Gamma \lesssim 1$ and $b_\Gamma = 6$.

Because typical plasma dynamical equations are quadratically nonlinear, $\partial_t \psi + \dots = \frac{1}{2} M \psi \psi$, one might expect that quadratic products such as $\tilde{\Gamma}$ would possess statistics similar to those observed. The fundamental difficulty is that nonlinearity precludes Gaussianity; the product of two Gaussian r.v.’s is not Gaussian. Since the fluctuations evolve self-consistently and nonlinearly, Gaussian statistics at one time step are transformed into non-Gaussian ones at the next. Thus the jointly Gaussian assumption for \tilde{x} and \tilde{y} cannot be correct. Also, the $\tilde{\Gamma}$ model predicts nonzero K for vanishing S ; one has $S_\Gamma(0) = 0$ and $K_\Gamma(0) = 6$. This is reminiscent of vari-

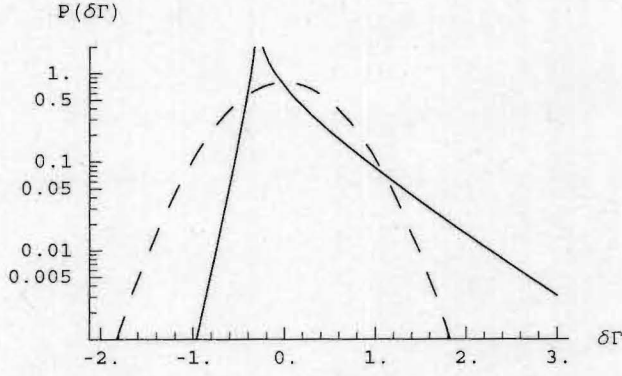


FIG. 3: Solid curve: PDF of the flux fluctuations $\delta\Gamma \doteq \Gamma - \langle \Gamma \rangle$ for $\rho = 0.75$. Dashed curve: reference Gaussian with same variance (the same as used in Fig. 4).

ous dynamical models with special symmetries (e.g., the Hasegawa–Wakatani system),⁸ and Figs. 1 and 2 include such points; however, the value of b_Γ is clearly too large. Of course, one would not expect vanishing ρ for a $\psi\psi$ nonlinearity. Coincidentally, $K_\Gamma(1)/S_\Gamma^2(1) = \frac{3}{2}$. However, although simple models like $\tilde{\Gamma} = \tilde{x}\tilde{y}$ may capture some part of the truth, they have no dynamical content. A similar difficulty afflicts attempts to fit results to other well-known PDFs, as was done in Ref. 1.

SS considered the nonlinear Langevin equation

$$\partial_t \tilde{\psi}(t) + \lambda \tilde{\psi} + \sigma_V (\tilde{f}\tilde{\psi} - \langle \tilde{f}\tilde{\psi} \rangle) = \sigma_f \tilde{f}(t) + \sigma_r \tilde{r}(t) \quad (1)$$

(in the Stratonovich interpretation), where \tilde{f} (forcing by wind) and \tilde{r} (residual effects) are Gaussian white noise with unit strength and the σ 's are strength parameters. (The subscript V in σ_V stands for velocity.) The associated Fokker–Planck equation for $P(\psi, t)$ is

$$\frac{\partial P}{\partial t} = \frac{\partial}{\partial \psi} (\lambda_{\text{eff}} \psi P) + \frac{1}{2} \frac{\partial^2}{\partial \psi^2} \{[(\sigma_f - \sigma_V \psi)^2 + \sigma_r^2] P\}, \quad (2)$$

where $\lambda_{\text{eff}} \doteq \lambda - \frac{1}{2}\sigma_V^2$. Although the steady-state solution of Eq. (2) can be determined analytically (see Fig. 4, which clearly shows the skewness and flatness), it is too complicated for further manipulations. SS followed the alternate approach of deducing recursion equations for the moments. One has $\langle \psi \rangle = 0$ and

$$\left(\lambda_{\text{eff}} - \frac{1}{2}(n-1)\sigma_V^2 \right) \langle \psi^n \rangle = -(n-1)\sigma_V \sigma_f \langle \psi^{n-1} \rangle + \frac{1}{2}(n-1)(\sigma_f^2 + \sigma_r^2) \langle \psi^{n-2} \rangle. \quad (3)$$

Upon eliminating the variance $\langle \psi^2 \rangle$ between the $n = 3$ and $n = 4$ equations, SS were led to the basic result $K = aS^2 + b$ with known formulas for $a(\sigma_V)$ and $b(\sigma_V)$. One has $a(0) = \frac{3}{2}$, $b(0) = 0$, and $a(\sigma_V) > a(0)$; these provide a reasonable description of the SST data.

In view of the similarity between the TORPEX and SST datasets, it is appropriate to ask whether the SS model applies to TORPEX. The answer is far from

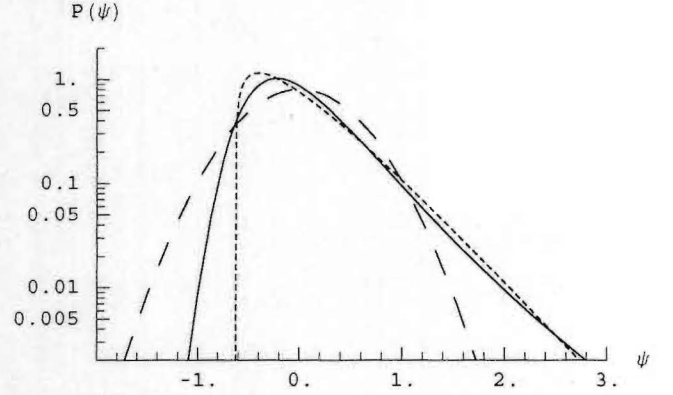


FIG. 4: Solid curve: example of the steady-state PDF ($\lambda = 1$, $\sigma_f = 0.50$, $\sigma_r = 0.35$, $\sigma_V = 0.5$); note the skewness and the general similarity to Fig. 3. Dotted curve: Beta PDF with identical skewness ($S = 1.6$). Dashed curve: reference Gaussian. All curves have identical mean (0) and standard deviation (0.50).

clear. SS considered fluctuations that were forced externally, whereas the plasma turbulence is self-excited. Furthermore, linear waves can be important in D-I turbulence but were not considered by SS.

Further discussion about the interpretation of such nonlinear L models is given below. First, I describe a primitive attempt to generalize Eq. (1) to include wave effects. Specifically, instead of considering the real scalar field $\tilde{\psi}$, I consider two real amplitudes \tilde{A} and \tilde{B} , coupled only through linear terms such that the eigenvalues for $\lambda = 0$ are $\pm i\Omega$. Thus, I study

$$\begin{aligned} \frac{\partial}{\partial t} \begin{pmatrix} \tilde{A} \\ \tilde{B} \end{pmatrix} + \begin{pmatrix} \lambda & -\Omega \\ \Omega & \lambda \end{pmatrix} \cdot \begin{pmatrix} \tilde{A} \\ \tilde{B} \end{pmatrix} + \begin{pmatrix} \sigma_V (\tilde{f}_A \tilde{A} - \langle \tilde{f}_A \tilde{A} \rangle) \\ \sigma_V (\tilde{f}_B \tilde{B} - \langle \tilde{f}_B \tilde{B} \rangle) \end{pmatrix} \\ = \sigma_V \begin{pmatrix} \tilde{f}_A \\ \tilde{f}_B \end{pmatrix} + \sigma_r \begin{pmatrix} \tilde{r}_A \\ \tilde{r}_B \end{pmatrix}. \end{aligned} \quad (4)$$

The goal is to assess to what extent the presence of a real frequency significantly affects the relationship between S and K . (In reality, nonzero Ω modifies the nonlinear terms as well; *omitting that effect is an important deficiency of the present calculation.*)

Equation (4) leads to the Fokker–Planck equation

$$\begin{aligned} \partial_t P(A, B, t) \\ = \left(\frac{\partial}{\partial A} [(\lambda_{\text{eff}} A - \Omega B) P] + (A, \Omega \leftrightarrow B, -\Omega) \right) \\ + \frac{1}{2} \left(\frac{\partial^2}{\partial A^2} \{[(\sigma_f - \sigma_V A)^2 + \sigma_r^2] P\} + (A \leftrightarrow B) \right). \end{aligned} \quad (5)$$

In steady state, equations for the moments $\langle \tilde{A}^{n-m} \tilde{B}^m \rangle$ ($0 \leq m \leq n$) through order $n = 4$ can be obtained. They have the structure $\langle \tilde{A} \rangle = \langle \tilde{B} \rangle = 0$, $\langle \tilde{A} \tilde{B} \rangle = 0$, and

$$\langle \tilde{A}^2 \rangle = \langle \tilde{B}^2 \rangle = \bar{A}^2 \doteq (\sigma_f^2 + \sigma_r^2) / [2(\lambda - \sigma_V^2)], \quad (6a)$$

$$M_{44} \cdot \langle \tilde{\psi}_4 \rangle = \bar{A}^2 \sigma_V \sigma_f M_{41}, \quad (6b)$$

$$M_{55} \cdot \langle \tilde{\psi}_5 \rangle = \sigma_V \sigma_f M_{54} \cdot \langle \tilde{\psi}_4 \rangle + \bar{A}^2 (\sigma_f^2 + \sigma_r^2) M_{51}, \quad (6c)$$

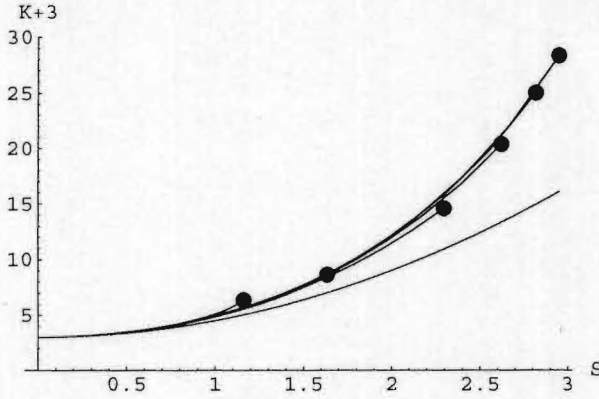


FIG. 5: Predictions of the generalized stochastic model for $\sigma_f = 1$ and $\sigma_r = 0$. Each black curve represents a particular frequency Ω , with $S(\Omega, \sigma_V)$ and $K(\Omega, \sigma_V)$ scanned over the range $0 \leq \sigma_V \leq 0.6$. The successively shorter curves (end points indicated by filled circles) represent $\Omega = 0$ (the basic SS model), 0.25, 0.5, 1, 2, and 3. The lowest curve is $K = \frac{3}{2}S^2$.

where, e.g., $\langle \tilde{\psi}_4 \rangle \doteq (\langle \tilde{A}^3 \rangle, \langle \tilde{A}^2 \tilde{B} \rangle, \langle \tilde{A} \tilde{B}^2 \rangle, \langle \tilde{B}^3 \rangle)^T$ and the M 's are known matrices (dependent on λ , Ω , and σ_V). If one defines $S \doteq \langle \tilde{A}^3 \rangle / \bar{A}^3$ and $K \doteq \langle \tilde{A}^4 \rangle / \bar{A}^4 - 3$, one is led to the relation $K = aS^2 + b$ with specific formulas for $a(\lambda, \Omega, \sigma_V)$ and $b(\lambda, \Omega, \sigma_V)$, e.g.,

$$a = (M_{55}^{-1} \cdot M_{54} \cdot M_{44}^{-1} \cdot M_{41})[1] / \{(M_{44}^{-1} \cdot M_{41})[1]\}^2. \quad (7)$$

Alternatively, one can obtain parametric plots of K vs. S by varying σ_V with all other parameters fixed. An example is shown in Fig. 5, which should be compared with Fig. 1. It is seen that the principal effect of nonzero Ω is to limit the maximum values of S and K . That is consistent with the tendency of the data points in Fig. 1 to cluster near the bottom of the parabola. (Those points are associated with regions of TORPEX in which D-I turbulence is expected to be operating.)

In Refs. 1 and 2, it was concluded that the beta PDF P_β provided a very good fit to the data. In Fig. 4 I compare the predictions of the L PDF P with the P_β possessing the same mean, standard deviation σ , and skewness. (I use the $\Omega = 0$ form of the theory, but Fig. 5 shows that the S and K should be essentially the same for $\Omega \approx 1$.) The right-hand tails, which dominate K , are almost identical. (For P_β , K_β is slightly less than $\frac{3}{2}S_\beta^2$, whereas for P K is slightly higher than $\frac{3}{2}S^2$.) The principal difference is obviously the sharp cutoff of P_β at some ψ_{\min} . The L theory does not attempt to constrain the size of the fluctuations (in density n , say), whereas in reality the total n must be positive. However, Fig. 5 corresponds to a rather large σ , $\langle \psi^2 \rangle^{1/2} = 0.50$. For smaller σ , the effect of the constraint would be less. (Also, the shaping of the left-hand tail can be changed by adjusting σ_r .) Thus, the predictions of the L theory are not unreasonable, and it has a dynamical basis.

I will now attempt an interpretation of such models, considering the $\Omega = 0$ case for simplicity. I begin by assuming homogeneous statistics and the primitive ampli-

tude equation $\partial_t \psi_k - \gamma_k \psi_k = \frac{1}{2} \sum_{\Delta} M_{k,p,q} \psi_p^* \psi_q^* + \tilde{f}_k^{\text{ext}}$, where $\sum_{\Delta} \doteq \sum_{p,q} \delta_{k+p+q}$. The general theory of statistical closure⁴ provides two important motivations. First, in formally exact renormalized spectral balances the effects of a quadratic nonlinearity are represented by two distinct terms: a ‘‘coherent’’ damping η_k^{nl} (typically positive as a function of wave number k), and the variance F_k^{nl} of an ‘‘incoherent’’ forcing \tilde{f}_k^{nl} . For example, a Markovian spectral balance equation for equal-time covariance C_k is

$$\frac{1}{2} \partial_t C_k - \gamma_k C_k + \eta_k^{\text{nl}} C_k = F_k^{\text{nl}} + F_k^{\text{ext}}. \quad (8)$$

Second, realizable L representations are known for important closures such as the DIA and the EDQNM (see Ref. 4 and references therein). For example, the L representation of the $\Omega = 0$ EDQNM¹³ is

$$\partial_t \tilde{\psi}_k(t) - \gamma_k \tilde{\psi}_k + \eta_k^{\text{nl}} \tilde{\psi}_k = \tilde{f}_k^{\text{nl}}(t) + \tilde{f}_k^{\text{ext}}(t), \quad (9a)$$

$$\tilde{f}_k^{\text{nl}}(t) \doteq \frac{1}{2} \tilde{w}(t) \sum_{\Delta} M_{k,p,q} (\theta_{k,p,q})^{1/2} \tilde{\xi}_p^*(t) \tilde{\xi}_q^*(t), \quad (9b)$$

where $\tilde{w}(t)$ is Gaussian white noise with unit diffusion coefficient, the $\tilde{\xi}$'s are Gaussian r.v.'s with covariance equal to that of the predicted $\tilde{\psi}$, and $\theta_{k,p,q}$ is the triad interaction time. A formula is also given for η_k^{nl} such that energy is conserved by the nonlinear terms. The role of \tilde{w} is to ensure a Markovian description of the statistics.

The measured statistics are calculated from x -space quantities, which are built from many Fourier amplitudes. However, the $\Omega = 0$ L model considers just a single variable, which must thus be interpreted as the amplitude of a typical wave number in the energy-containing range. Note that linear dissipation is typically small for such k 's; nonlinear mode coupling transfers energy to other k 's where it is dissipated. Therefore, the λ parameter should be interpreted not as linear dissipation but rather as the coherent nonlinear damping η^{nl} . No growth-rate term is apparent in the L model. That has been modeled by Gaussian forcing \tilde{f}^{lin} (a common artifice); one recovers the L model by defining $\tilde{f} \doteq \tilde{f}^{\text{lin}} + \tilde{f}^{\text{ext}}$. The $\sigma_V \tilde{f} \tilde{\psi}$ term of Eq. (1) apparently models \tilde{f}^{nl} [cf. formula (9b)]. This interpretation is consistent with the result (6a) for the steady-state fluctuation level, which demonstrates a balance between stochastic forcing and $\hat{\lambda} \doteq \lambda - \sigma_V^2$, not λ . $\hat{\lambda}$ measures the difference between the coherent damping and incoherent forcing; cf. the combination $\eta_k^{\text{nl}} C_k - F_k^{\text{nl}}$ in Eq. (8). That is, $\hat{\lambda}$ measures the nonlinear transfer out of the forced k 's. That must be equal to the net dissipation, which shows up as the denominator in Eq. (6a). This argument suggests that the residual \tilde{r} is inessential, and indeed better agreement with the observed ranges of S and K is obtained by setting $\sigma_r = 0$.

One must also discuss why it is \tilde{f} rather than some other random function that is used in the nonlinear term of the L models. Temporarily suppose that $\tilde{f}^{\text{ext}} = 0$ and recall the interpretation of the nonlinear term as $\mathbf{E} \times \mathbf{B}$ advection. For example, the polarization-drift nonlinearity (advection of vorticity) is $\tilde{\mathbf{V}}_E \cdot \nabla (\nabla^2 \tilde{\varphi})$, with $\tilde{\varphi}$ being

the electrostatic potential and $\tilde{V}_E \doteq \hat{z} \times \nabla \tilde{\varphi}$ in suitably dimensionless variables. Now in general the statistics of a field and its gradient differ. However, the gradient of a Gaussian field is again Gaussian. The linear forcing has been modeled by $\gamma \tilde{\varphi} \rightarrow \tilde{f}^{\text{lin}}$. At that point, one is assuming that $\tilde{\varphi}$ is Gaussian; to that extent, \tilde{V}_E would be Gaussian as well. Also, \tilde{V}_E should increase with \tilde{f}^{lin} .

Such arguments may provide motivation, but they stretch the truth in many ways. Both the true dynamics and the L solution are non-Gaussian; thus neither $\gamma \tilde{\varphi}$ nor \tilde{V}_E are Gaussian, nor are they white. All details of nonlinear mode coupling as well as the difference between a self-consistently determined \tilde{f}^{lin} and an externally specified \tilde{f}^{ext} have been completely swept under the rug. Furthermore, a complete interpretation must probably address inhomogeneous statistics (e.g., by including a self-consistently determined background profile), since special symmetries of homogeneous systems may constrain S , but not K , to vanish.⁸ The nonlinear L model does capture the tendency of the turbulence amplitude to scale with the forcing (essentially the argument of SS). But all in all, the model could hardly be more naive. At some level, it seems that it may be enough. However, nothing has been proven; a proper assessment of the merits of such an approach, an investigation of the relative roles of internal and external forcing, and further insight into the role of inhomogeneity must be left to future work. K - S plots from other machines and numerical studies of various nonlinear systems would be very desirable.

One can contemplate more sophisticated models in which the mode coupling is handled realistically. However, even cursory study of Ref. 6, in which the structure of fourth-order cumulant-based statistical models is discussed, is sufficient to show that the analysis would be extremely formidable; note that even solutions of the realizable Markovian closure⁹ for second-order Hasegawa-Mima¹⁰ or Hasegawa-Wakatani¹¹ statistics were entirely nontrivial. An important alternative is the PDF-based mapping closure.¹² However, implementation of mapping

closure for problems involving linear waves and, possibly, coupled fields is not well understood.

One may question whether it is even necessary to pursue complicated analytical models that attempt to be more faithful to the nonlinear dynamics. x -space statistics are constructed from sums over many Fourier modes, each of which has a different detailed response, so a kind of spectral averaging is performed that washes out some details. Statistics predicted by the generalized model discussed above are not strongly dependent on frequency, but the TORPEX data embraces various physics regimes that include both $\Omega = 0$ and $\Omega \neq 0$. Even the utterly simplest $\tilde{\Gamma}$ model predicts a nontrivial relationship between K and S . True, it does not agree with observations, but the slope $dK_{\Gamma}/d(S_{\Gamma}^2)$ differs at large correlation coefficient by only about 50% from the observations and simple nonlinear Langevin models. That is significant, but it is a “fuzzy,” quantitative error. It is not clear exactly what physics process would be discriminated by a theory that would predict that slope very accurately. A further complication is that it is not obvious to what extent non-Gaussian higher-order statistics affect important second-order quantities like turbulent fluxes. Second-order closures can make satisfactory predictions for turbulent transport even when the bulk of the fluctuations can be classified as “coherent structures.”¹¹

Nevertheless, analytical prediction of higher-order statistics and careful comparison of such theory with experimental observations are in the best tradition of probing deeply into nonlinear science. That the basic SS model and its modest frequency-dependent generalization make predictions that are not totally unreasonable gives one some hope that further tractable calculations may remain in this difficult and challenging field of statistical plasma/fluid dynamics.

This work was supported by U.S. Department of Energy Contract No. DE-AC02-76-CHO-3073. I am grateful for helpful discussions with G. Hammett, B. Labit, P. Sura, and S. Zweben.

* Electronic address: krommes@princeton.edu

¹ B. Labit, I. Furno, A. Fasoli, A. Diallo, S. H. Müller, G. Plyushchev, M. Podestà, and F. M. Poli, Phys. Rev. Lett. **98**, 255002 (2007), URL <http://link.aps.org/abstract/PRL/v98/e255002>.

² B. Labit, A. Diallo, A. Fasoli, I. Furno, D. Iraj, S. H. Müller, G. Plyushchev, M. Podestà, F. M. Poli, P. Ricci, et al., Plasma Phys. Control. Fusion **49**, B281 (2007).

³ P. Sura and P. D. Sardeshmukh, J. Phys. Oceanogr. **38**, 638 (2007).

⁴ J. A. Krommes, Phys. Rep. **360**, 1 (2002).

⁵ H. Chen, J. R. Herring, R. M. Kerr, and R. H. Kraichnan, Phys. Fluids A **1**, 1844 (1989).

⁶ J. A. Krommes, Phys. Rev. E **53**, 4865 (1996).

⁷ B. A. Carreras, C. Hidalgo, E. Sánchez, M. A. Pedrosa,

R. Balbín, I. García-Cortés, B. van Milligen, D. E. Newman, and V. E. Lynch, Phys. Plasmas **3**, 2664 (1996).

⁸ I am grateful to G. Hammett (private communication, 2008) for emphasizing this point.

⁹ J. C. Bowman, J. A. Krommes, and M. Ottaviani, Phys. Fluids B **5**, 3558 (1993).

¹⁰ J. C. Bowman and J. A. Krommes, Phys. Plasmas **4**, 3895 (1997).

¹¹ G. Hu, J. A. Krommes, and J. C. Bowman, Phys. Lett. A **202**, 117 (1995); Phys. Plasmas **4**, 2116 (1997).

¹² H.-D. Chen, S. Chen, and R. H. Kraichnan, Phys. Rev. Lett. **63**, 2657 (1989).

¹³ For $\Omega \neq 0$, subtle realizability issues arise; see the development of the realizable Markovian closure in Ref. 9.

The Princeton Plasma Physics Laboratory is operated
by Princeton University under contract
with the U.S. Department of Energy.

Information Services
Princeton Plasma Physics Laboratory
P.O. Box 451
Princeton, NJ 08543

Phone: 609-243-2750
Fax: 609-243-2751
e-mail: pppl_info@pppl.gov
Internet Address: <http://www.pppl.gov>